The Random Phase Transducer: A New Technique for Incoherent Processing—Basic Principles and Theory

MATHIAS FINK, RAOUL MALLART, AND FABRICE CANCRE

Abstract—**Speckle noise is a source of errors in envelope estimation and spectral analysis of pulse-echo signals. It is due to the coherent nature of the ultrasonic modality. This noise can be reduced through the use of incoherent processing techniques. The theoretical limit for the SNR improvement when incoherent processing techniques are used is studied. The study leads to the concept of information grain. A simple technique for incoherent processing that is easy to implement and that allows a good physical understanding of the limitations of incoherent processing of pulse-echo signals is also studied. This technique does not require the division of the receiving aperture into many small coherent subelements nor the scanning of the field as in spatial compounding, nor the use of low sensitivity CdS transducers. It involves a single coherent transducer and a moving random phase screen placed in front of it.**

I. Introduction

SPECTRAL ANALYSIS and envelope estimation are widely used tools in tissue characterization and in ultrasound imaging. They are used in measurement of backscattered field [1]–[3]. Their use for the estimation of the ultrasound attenuation as a function of frequency has been studied by many authors [4]–[6]. However, in multiscattering media such as biological tissue, interference between echoes from randomly located scatterers within the resolution cell lead to random errors in spectral estimation and speckle noise in envelope detection. This speckle noise is linked to the spatially coherent behavior of piezoelectric transducers. Indeed in a piezoelectric transducer, the pulse-echo signal depends on the instantaneous force applied to its front surface. Thus, the generated signal results from a linear summation over the whole transducer surface of the scattered pressure wave. Statistics of this noise have been studied by many authors in the ultrasound domain [7]–[10] as well as in optics where a similar problem exists [11], [12].

The problem of speckle reduction can be approached by several ways. One of them involves signal processing or image processing such as adaptive filtering techniques [13]. This approach is interesting but is out of the scope of this paper. Another approach (that is studied here) involves physical principles.

It is generally accepted that the speckle results from the coherent summation of random phasors and that an ultrasonic image is a particular realization of a stochastic process. The intensity value of a particular pixel on an ultrasonic image is therefore considered to be a random variable whose value depends on an interference pattern. If we can generate another image of the same medium with different interference patterns, we will have another realization of the random variable. Averaging of the images will result in a reduction of the speckle. The basic principle in this approach is the averaging of realizations of a same random process. Maximal efficiency is obtained when the different realizations are uncorrelated. This approach is called incoherent processing of pulse-echo signals.

Spatial compounding and frequency compounding are two such techniques. In spatial compounding [7], [14], [16], the data to be averaged are obtained by scanning the transducer through the field. The medium to be imaged is viewed from different angles and it is easy to understand why it yields different interference patterns. In frequency compounding [17], [18] the illumination beam contains different frequencies. At each frequency, a different interference pattern is obtained.

A similar approach consists in sampling the field with small-aperture piezoelectric elements laid out in a two-dimensional (2-D) array or pseudoarray [3], [19]. Intensity, or envelope-detected echoes from the array elements are averaged. (Averaging of the power spectra may also be performed). This approach is also called phase insensitive detection. Power-sensitive receivers such as the acoustoelectric transducer made of CdS [20] can be used to replace the array. However, these transducers exhibit a lack of sensitivity.

In this paper, we study the theoretical limits of incoherent processing of quasi-monochromatic pulse-echo

Manuscript received March 27, 1989; revised September 18, 1989; accepted September 20, 1989.

M. Fink is with the Groupe de Physique des Solides de l'ENS, Université Paris 7, 2 Place Jussieu, 75251 Paris, Cedex 05, France.

R. Mallart is with the Groupe de Physique des Solides de l'ENS, Université Paris 7, 2 Place Jussieu, 75251 Paris, Cedex 05, France, and with the Laboratoire d'Electronique Philips, 3 Avenue Descartes, 94451 Limeil-Breuannes, France.

F. Cancre is with the Groupe de Physique des Solides de l'ENS, Université Paris 7, 2 Place Jussieu, 75251 Paris, Cedex 05, France, and with the Laboratoires d'Electronique Philips, 3 Avenue Descartes, 94451 Limeil-Breuannes, France.

IEEE Log Number 8933095.

signals. (Frequency compounding is out of the scope of this study). We also present a new approach that yields spatial incoherence. For this method, there is no need of dividing the receiving aperture into subelements, or of scanning the field.

This technique requires only one transducer filling the entire receiving aperture. The spatial coherence is controlled by moving a random phase screen that is placed across the beam of the transducer [21]. Envelope detection or spectral analysis are then performed for each position of the random phase screen. The averaging of these data is then performed on a set of screen positions. Similar devices have already been used in ultrasonic imaging [22], [23]. However, they are based on a different approach of the imaging process. The system described by Sato *et al.* [22] is based on a transmission imaging where the ultrasonic "shadow" of the object to be imaged is transformed into a random time series by the moving random phase screen. The image in then reconstruct from the time series. The technique described by Röder *et al.* [23] is also based on transmission imaging. They use a random phase device in order to simulate an incoherent ultrasonic source analog to an incoherent light source.

II. Limitations of Incoherent Processing

A. A Simple Incoherent Processing Theory

As an ultrasonic beam illuminates an inhomogeneous medium, a pressure field is scattered towards the receiving transducer. In order to get a good physical understanding of pulse–echo processes, we model the receiving transducer as a continuous set of piezoelectric points. At time t, each point $\vec{X}$ of the transducer plane intercepts a set of spherical wavelets coming from the scatterers located in the isochronous volume. In the special (and simple) case of a uniform plane-wave illumination, the pressure signal observed at $\vec{X}$ can be written as

$$p(\vec{X}, t) = \sum_{i \in \text{scatterers}} p_i(\vec{X}, t) \tag{1}$$

where $p_i(\vec{X}, t)$ corresponds to the elementary pressure signal scattered by scatterer i and received in $\vec{X}$.

Such a pressure signal is random. The integrated pressure over the receiver (whose aperture function is $O_r(\vec{X})$) is the coherent pulse–echo signal

$$e_{\text{coh}}(t) = \int O_r(\vec{X})\, p(\vec{X}, t)\, d\vec{X}. \tag{2}$$

The signal e_{coh} is also random and in the limiting case of a monochromatic illumination, it gives rise to the classical speckle theory that predicts quite low signal-to-noise ratio (SNR) (in the sense of ensemble statistics) of 1.0 and 1.91 respectively for intensity and envelope detected signals [7]–[9].

In an analogy to the optical modality, where the receivers are sensitive to the integrated pressure intensity over the response time of the detectors, we now assume that the receiver generates a signal proportional to the total acoustic power it receives rather than to the integrated acoustic force. Such transducers can be built, as it was mentioned earlier, in CdS [20], or can be simulated by the use of piezoelectric arrays or (pseudoarrays) [3]. The output signal is the incoherent pulse–echo signal

$$e_{inc}(t) = \int O_r(\vec{X})\, a^2(\vec{X}, t)\, d\vec{X} \tag{3}$$

where a^2 is the square-detected pressure signal. It is defined through the well-known relation

$$p(\vec{X}, t) = a(\vec{X}, t) \cos \phi(\vec{X}, t) \tag{4}$$

where ϕ is the instantaneous phase and a is the envelope. This decomposition of a signal into its envelope and phase is classical and relates to the concept of analytic function associated to a real function.

A major disadvantage of this technique is that it does not allow focusing in receive mode. Indeed, in a coherent piezoelectric transducer, focusing results from the coherent summation of properly phase shifted signals.

In order not to lose too much lateral resolution, it is better to divide the receiving aperture into larger coherent subelements. This scheme is used for example in the Maltese cross processor [19] where the receiver is divided into 32 sectors. It is understood that the larger the coherent subelements, the better the resolution. The optimal size of these subelements depends on the statistical properties of the scattered field. This can be easily understood if incoherent processing techniques are viewed as averaging techniques. Spatial and frequency compounding as well as the Maltese cross processor are based on averaging on an intensity basis. To reduce the speckle noise, we need to average uncorrelated data. Therefore, optimal processing is obtained when the data from different subelements are uncorrelated. This was extensively investigated for spatial compounding techniques [10], [16].

In this paper we use a different approach. We want to know the number of uncorrelated data that can be collected on a given receiving aperture and the maximal size of subelement that still yields uncorrelated data. This is important for the optimization of the subelement size in incoherent processing: Dividing the receiving aperture into very small coherent elements is not efficient because they have a poor directivity and many of them yield correlated data. On the other hand, dividing it into large elements does not reduce efficiently the speckle noise. The study of this compromise requires the knowledge of the scattered field autocorrelation function on the plane of the receiver. The optimal size of the subelements will be related to the width of the scattered field autocorrelation function.

B. The Scattered Field Autocorrelation

In the following, we introduce an approximation that greatly simplifies the theoretical approach to pulse echo processing. We assume that the pressure fields are quasi-monochromatic (continuous wave approximation). This approximation is partly justified because the behavior of pulse–echo signals are strongly linked to their mean fre-

quency. Furthermore, experimental results confirm the validity of this approximation.

This approximation is useful mainly because it eliminates the time dependence of the pressure fields. A monochromatic pressure field $p(\vec{X}, t)$ can be totally described in terms of its amplitude $A(\vec{X})$, its phase $\Phi(\vec{X})$ and its frequency ω. The amplitude and phase can be combined to form the complex amplitude $P(\vec{X})$:

$$P(\vec{X}) = A(\vec{X})e^{j\Phi(\vec{X})}. \tag{5}$$

The pressure field is obtained from its complex amplitude and through the relation

$$p(\vec{X}, t) = Re\left\{P(\vec{X})e^{-j\omega t}\right\}. \tag{6}$$

Therefore, once the frequency is set, the pressure field is completely described by its complex amplitude. Through the text, P is used for the complex amplitude of the pressure fields, while p is used for the real time dependent pressure fields. More generally, capital letters are used for complex amplitude signals while low case letters for the real, time dependent, signals.

The scattering medium is modeled as a random distribution of scatterers located in the insonified volume. In pulse–echo processing, the scattering volume is divided into elementary slices whose thickness is equal to the axial resolution cell. Under the monochromatic approximation, it is interesting to model the slice of scattering medium as a 2-D random mirror. This model is described in the appendix. Note however that such a random mirror only describes a thin slice of the scattering medium. For each depth, a different random mirror has to be defined.

Let's call P_i the complex amplitude of the incident pressure field on the random mirror and P_r the complex amplitude of the pressure field reflected by the random mirror. P_i describes the illumination beam on the plane of the random mirror. The ratio between P_r and P_i defines the reflectance r of the mirror. At position $\vec{x}$ on the plane of the random mirror, we have

$$P_r(\vec{x}) = r(\vec{x})\, P_i(\vec{x}). \tag{7}$$

The reflectance $r(\vec{x})$ is a complex random function. In the realistic case where the scattering medium is uncorrelated (totally random) and contains a large number of scatterers per resolution cell, $r(\vec{x})$ is a Gaussian random function and its autocorrelation function is proportional to a Dirac function.

Note that coordinates on the plane of the random mirror are noted $\vec{x}$, while coordinates on the plane of the transducers are noted $\vec{X}$.

Since $r(\vec{x})$ is a random function, $P_r(\vec{x})$ is also a random function. Its autocorrelation function is

$$R_{P_r}(\vec{x}_2, \vec{x}_1) = P_i(\vec{x}_2)\, P_i^*(\vec{x}_1)\, R_r(\vec{x}_2, \vec{x}_1). \tag{8}$$

Since the scattering medium is assumed to be uncorrelated, the above expression is equivalent to

$$R_{P_r}(\vec{x}_2, \vec{x}_1) = P_i(\vec{x}_2)\, P_i^*(\vec{x}_1)\, \delta(\vec{x}_2 - \vec{x}_1). \tag{9}$$

The diffracted wavefield originating from such a random mirror propagates as a complex random field whose phase and amplitude fluctuate in space. The scattered pressure field $P(\vec{X})$ observed on the plane of the receiver is obtained from the Huygens–Kirchoff formulation. In the Fresnel approximation, it can be reduced to the Fresnel transform of $P_r(\vec{x})$, which is defined by [24]

$$P(\vec{X}) \propto \int d\vec{x}\; P_r(\vec{x}) \exp\left(\frac{j\pi}{\lambda z}\,|\vec{x} - \vec{X}|^2\right) = P_r(\vec{X}) \otimes \exp\left(\frac{j\pi}{\lambda z}\,|\vec{X}|^2\right) \tag{10}$$

where $\otimes$ is the convolution product and z the depth of the considered slice of scattering medium.

Our objective is to compute the autocorrelation function of the complex pressure field $P(\vec{X})$ on the plane of the receiver. That is, the autocorrelation of the output of a linear system whose impulse response is $\exp[(j\pi/\lambda z)|\vec{x}|^2]$ and whose input is $P_r(\vec{x})$. From linear system theory ([25, p. 286]), we have

$$\begin{aligned} R_P(\vec{X}_2, \vec{X}_1) &= R_{P_r}(\vec{X}_2, \vec{X}_1) \otimes \exp\left(-\frac{j\pi}{\lambda z}\,|\vec{X}_1|^2\right) \otimes \exp\left(\frac{j\pi}{\lambda z}\,|\vec{X}_2|^2\right) \\ &= |P_i(\vec{X}_1)|^2 \exp\left(-\frac{j\pi}{\lambda z}\,|\vec{X}|^2\right) \otimes \exp\left(\frac{j\pi}{\lambda z}\,|\vec{X}|^2\right) \end{aligned} \tag{11}$$

where $\vec{X} = \vec{X}_2 - \vec{X}_1$. This can be rewritten, as the Fourier transform of $|P_i(\vec{X}_1)|^2$ taken at the spatial frequency $\vec{X}/\lambda z$:

$$R_P(\vec{X}_2, \vec{X}_1) = \exp\left[\frac{j\pi}{\lambda z}\left(|\vec{X}_2|^2 - |\vec{X}_1|^2\right)\right] \cdot \mathrm{FT}\left(|P_i(\vec{X}_1)|^2\right)\left(\frac{\vec{X}}{\lambda z}\right). \tag{12}$$

The aforementioned phase factor can be ignored in the study of backscattered field autocorrelation width. In the following, we ignore the phase factor and thus, we can consider that R_p is a function of $\vec{X} = \vec{X}_2 - \vec{X}_1$.

$$R_P(\vec{X}_2, \vec{X}_1) \simeq \mathrm{FT}\left(|P_i(\vec{X}_1)|^2\right)\left(\frac{\vec{X}}{\lambda z}\right). \tag{13}$$

1) Focused Transducer: In the case where the transmitting transducer is focused, the incident pressure field on the focal plane $P_i(\vec{x})$ is the Fourier transform (FT) of the transducer aperture function $O_t(\vec{x})$

$$P_i(\vec{x}) = \mathrm{FT}\left(O_t(\vec{X})\right)\left(\frac{\vec{x}}{\lambda F}\right). \tag{14}$$

From the above derivation, we deduce that the scattered field autocorrelation function observed at a distance z from

the random mirror is equal to

$$R_P(\vec{X}) \simeq \mathrm{FT}\left(\left|P_i(\vec{x})\right|^2\right)\left(\frac{\vec{X}}{\lambda z}\right), \tag{15}$$

which reduces, in the case where $z = F$ to

$$R_P(\vec{X}) \simeq \mathrm{FT}\left\{\left|\mathrm{FT}(O_t)\left(\frac{\vec{x}}{\lambda F}\right)\right|^2\right\}\left(\frac{\vec{X}}{\lambda z}\right). \tag{16}$$

From the Wiener–Kinchine theorem, we have

$$R_P(\vec{X}) \propto R_{O_t}(\vec{X}). \tag{17}$$

The scattered field autocorrelation function is proportional to the transmitting aperture autocorrelation function. Therefore, if the transmitting and receiving apertures have the same size, we receive a very limited amount of uncorrelated data. It is shown later on that for incoherent processing and when the same aperture is used in both transmission and reception, the maximal SNR improvement we can achieve is $\sqrt{2}$ for a 1-D focusing process (linear array), or 1.94, for a 2-D focusing process (circular transducer).

Better SNR improvements can be achieved by using a larger receiving aperture. We show later on that the number of uncorrelated data we can receive is a function of the ratio of the receiving aperture area to the transmitting aperture area.

2) Disc Plane Transducer: In the case where the transmitting transducer is a plane disc of radius a, the beam width is larger than in the focused case. It is well known that up to the Fresnel distance ($z_F = a^2/\lambda$), the incident pressure field is collimated in the transducer shadow. Therefore, P_i can be considered to be approximately proportional to the aperture function O_t of the transducer. Indeed this is a strong approximation but it allows a simple determination of the scattered field autocorrelation width. $R_p(\vec{X})$ can be approximated, with this assumption, as

$$R_P(\vec{X}) \propto \mathrm{FT}\left(\left|O_t(\vec{x})\right|^2\right)\left(\frac{\vec{X}}{\lambda F}\right). \tag{18}$$

The size of the scattered field autocorrelation is then dependent on the distance z from the random mirror and on λ the wavelength.

For a plane disc the aperture function is Circ ($|\vec{X}|/a$), therefore $|O_t(\vec{X})|^2 = O_t(\vec{X})$, and

$$R_p(\vec{X}) \propto \frac{J_1(\pi a|\vec{X}|/\lambda z)}{\pi a|\vec{X}|/\lambda z}. \tag{19}$$

The scattered field autocorrelation function at a depth z from the random mirror has a circular symmetry and is described by a Jinc function. Its transverse dimension (i.e., the coherence length of the scattered field) is about $\lambda z/D$ where D is the transducer diameter ($D = 2a$).

The number of uncorrelated data the receiver senses is approximately the ratio of its area to the field autocorrelation area. If the receiver diameter is also D, the number of uncorrelated data it senses is $(D^2/\lambda z)^2$. Therefore the maximal SNR improvement is about $D^2/\lambda z$. In the realistic case of a circular transducer of diameter 10 mm, working at 5 MHz and, considering a slice of medium placed at 40 mm, the SNR improvement is about 8.

3) Information Grains: Underlying to these findings is the concept of information grains. The size of an information grain is of the same order that the coherence length of the scattered field. The number of received information grains is proportional to the square of the SNR improvement. This theory is independent of the method used to achieve incoherence, and sets the limits for the SNR improvement.

This theory shows that the use of completely incoherent transducers is not a very efficient way of reducing speckle. Since only a few uncorrelated data can be received, it is better to divide the receiving transducer into coherent subelements whose sizes are well matched to the grain size. In that way, the maximal SNR improvement can still be achieved and the loss in lateral resolution is not as drastic.

One way of implementing a good incoherent transducer would be to build an array whose elements can be grouped in coherent subapertures. To achieve a maximal efficiency, 2-D processing should be preferred. However, such 2-D arrays are quite difficult to build. In the next section, we present another approach to incoherent processing of pulse echo signals.

III. A New Approach to Incoherent Pulse–Echo Processing

A. Principle

In this section, we study a new technique that also performs incoherent processing of pulse–echo signals. It consists in using a coherent transducer filling the entire receiving aperture. The degree of spatial coherence is controlled by moving a random phase screen (RPS) in front of the receiver. Envelope detection or spectral analysis are performed on the echographic lines recorded for each RPS position. Averaging of these data is then performed over a set of RPS positions.

The RPS generates random phase shifts that depend on its position and on the coordinates on the plane of the RPS. These random phase jitters are superimposed on the natural phase relationships between different points of the scattered field. The final effect is to destroy the phase information contained in the scattered field.

Two configurations can be thought of. They are illustrated in Fig. 1. The simplest one consists in using the same transducer in both transmit and receive modes. In that case, the RPS is in front of the transducer in both modes. In the other configuration, the RPS is present in receive mode only. This can be implemented for example if we use different transducers in the transmit and in the receive modes, or if the receiver is an array. In that case, the RPS can be simulated electronically. The theory presented here is developed for the second configuration (RPS

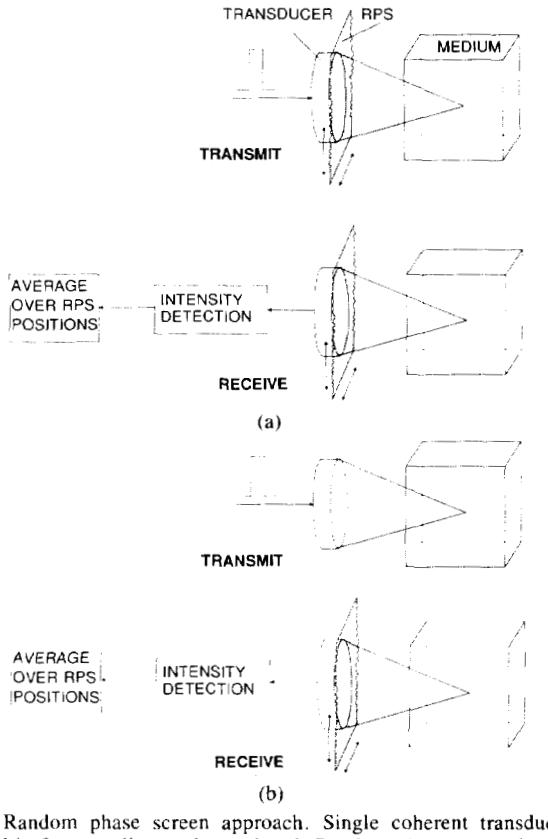

Fig. 1. Random phase screen approach. Single coherent transducer is placed in front medium to be explored. Random phase screen is moved across the beam of transducer. Envelope detection is performed for each position of the RPS. Detected lines are averaged over RPS positions. Two possible configurations are shown here. (a) RPS present in both transmit and receive modes. (b) RPS present in receive mode only.

in receive mode only). This simplification allows an easier understanding of the RPS technique and of the limits of incoherent transducers.

To get a good physical understanding of the limits of such transducers, one has to consider the properties of the RPS, the influence of its position, the directivity pattern of the incoherent transducer, the autocorrelation of the echo as well as the improvement in the SNR itself.

B. The Random Phase Screen

A random phase screen is a plane, nonattenuating, phase shift generating object. Practically it can be built as a plane object whose thickness varies with space and whose refraction index is different from the surrounding medium. Note that any aberrating medium (such as a fat layer of variable thickness) can be described by the model we introduce here.

The delaying (phase shifting) properties of the RPS are related to its roughness. Two functions characterize this roughness.

- The thickness distribution function. It characterizes the magnitude of the generated delays.
- The spatial autocorrelation function of the delays.

In this analysis, the thickness of the RPS is assumed to be a Gaussian random variable. Since the delays $\tau(\vec{X})$ are proportional to the thickness, their distribution is also Gaussian, and they can be assumed to have zero mean. Their variance will be noted σ_τ^2. We also assume that the spatial properties of the RPS are stationary and that the autocorrelation function of the delays, $R_\tau(\vec{X})$, is a Gaussian function with standard deviation σ_L.

1) Transmittance of the RPS: For any kind of screen, the transmittance can be defined locally as the ratio of the transmitted pressure field P_t to the incident pressure field P_i:

$$P_t(\vec{X}) = t(\vec{X})\, P_i(\vec{X}). \tag{20}$$

In the case of the previously defined, nonattenuating RPS, the thickness of the screen, $th(\vec{X})$ is a Gaussian random variable. Its autocorrelation function $R_{th}(\Delta\vec{X})$ is a Gaussian function defined as

$$R_{th}(\Delta\vec{X}) = \sigma_{th}^2 \exp\left(-\frac{|\Delta\vec{X}|^2}{2\sigma_L^2}\right), \tag{21}$$

where σ_L characterizes the roughness of the screen surface. The screen generates local phase shifts that are functions of the thickness and of the relative refraction index of the screen and of the coupling fluid ($n = c_{\text{fluid}}/c_{\text{screen}}$). The phase shifts can be written, if we ignore an additive constant, as

$$\Phi(\vec{X}) = 2\pi(n-1)\frac{th(\vec{X})}{\lambda}. \tag{22}$$

The associated time delays ($\tau(\vec{X}) = \Phi(\vec{X})/\omega$) are normally distributed. Without loss of generality, their mean can be ignored. Their autocorrelation function is

$$R_\tau(\Delta\vec{X}) = \sigma_\tau^2 \exp\left(-\frac{|\Delta\vec{X}|^2}{2\sigma_L^2}\right). \tag{23}$$

Now, the transmittance $t(\vec{X})$ of the screen is given by

$$t(\vec{X}) = e^{-j2\pi\tau(\vec{X})/T}, \tag{24}$$

where T is the acoustic period.

Now since $\tau(\vec{X})$ is a Gaussian random variable, we have

$$\langle t(\vec{X})\rangle = e^{-2\pi^2\sigma_\tau^2/T^2} \tag{25}$$

and

$$R_t(\Delta\vec{X}) = \exp\left[\frac{-4\pi^2\sigma_\tau^2}{T^2}\left[1 - \exp\left(-\frac{\Delta\vec{X}^2}{2\sigma_l^2}\right)\right]\right]. \tag{26}$$

As we will see later, we are interested in RPSs whose delay autocorrelation functions vanish when the shift $\Delta\vec{X}$ is large. To obtain such RPSs, relatively large σ_τ are required because that value sets the limit of $R_t(\Delta\vec{X})$, as $\Delta\vec{X}$ increases infinitely. Examples of RPS transmittance autocorrelation function are given in Fig. 2.

The width of $R_t(\Delta\vec{X})$ is strongly dependent on σ_L as well as on σ_τ. The larger σ_L and the smaller σ_τ, the wider $R_t(\Delta\vec{X})$.

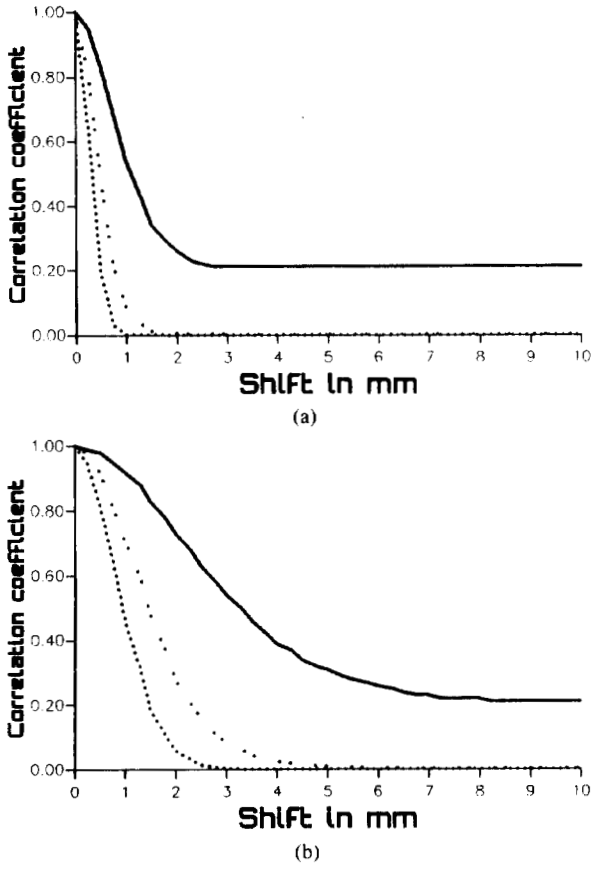

Fig. 2. RPS transmittance autocorrelation function where σ_r is as follows: 0.6 T for · · · · ·, 0.4 T for · · · · · ·, and 0.2 T for ——. (a) σ_L = 1 mm. (b) σ_L = 3 mm.

C. Equivalence Theorem

In this section, we show how our RPS-based approach is equivalent to the classical technique for incoherent pulse echo processing. This equivalence is true in the limiting case where the RPS is totally incoherent (i.e., its autocorrelation function is proportional to a Dirac function).

Let's consider $P(\vec{X})$, the complex pressure field sensed in $\vec{X}$ by the transducer without the RPS, and E the complex pulse-echo signal. We have

$$E = \int d\vec{X}\, O_r(\vec{X})\, P(\vec{X}). \tag{27}$$

Let's place a RPS on the surface of the transducer. According to (20), for a position δ of the screen, $P(\vec{X})$ becomes $P(\vec{X})\, t(\vec{X}, \vec{\delta})$ and the pulse-echo signal becomes

$$E_{\vec{\delta}} = \int d\vec{X}\, O_r(\vec{X})\, P(\vec{X})\, t(\vec{X}, \vec{\delta}). \tag{28}$$

Therefore, its squared magnitude is

$$|E_{\vec{\delta}}|^2 = \iint d\vec{X}_1\, d\vec{X}_2\, O_r(\vec{X}_1)\, O_r^*(\vec{X}_2)\, P(\vec{X}_2) \cdot P^*(\vec{X}_2)\, t(\vec{X}_1, \vec{\delta})\, t^*(\vec{X}_2, \vec{\delta}). \tag{29}$$

It is a random variable whose expectation with respect to the screen position is

$$\langle |E_{\vec{\delta}}|^2 \rangle = \iint d\vec{X}_1\, d\vec{X}_2\, O_r(\vec{X}_1)\, O_r^*(\vec{X}_2)\, P(\vec{X}_1) \cdot P^*(\vec{X}_2)\, R_t(\vec{X}_1 - \vec{X}_2). \tag{30}$$

Since R_t is proportional to a Dirac function and since $O_r = |O_r|^2$, we have

$$\langle |E_{\vec{\delta}}|^2 \rangle \propto \int d\vec{X}\, |O_r(\vec{X})|^2 |P(\vec{X})|^2 = \int d\vec{X}\, O_r(\vec{X}) |P(\vec{X})|^2. \tag{31}$$

The expectation of the square-detected pulse-echo signal is equal to the pulse echo produced by an incoherent transducer sensitive to the pressure intensity. Therefore, when we average the pulse echo signal through a totally incoherent RPS, our system is equivalent to a totally incoherent transducer such as those made out of CdS. Note that even though our system has a somewhat lower sensitivity than a classical coherent transducer [26], it has a higher sensitivity than transducers made of CdS, and may be an interesting alternative.

IV. Focused Transducer

The following analysis is restricted to the special case of the focused transducer, for which simple expressions in terms of Fourier transform exist for the directivity pattern in transmit and receive modes as well as for the echo. Note that similar relationships exist for the disc plane transducer, however, they involve Fresnel transforms and do not yield closed-form formulae.

A. Definition of the Directivity and of the Echo

Given a transducer and a RPS that acts only in receive mode, the directivity patterns in both transmit and in receive mode (respectively $U_t(\vec{x})$ and $U_r(\vec{x}, \vec{\delta})$) can be defined in terms of the aperture function of the transducer, O_t or O_r, and of the RPS transmittance t. Note that U_t represent the incident pressure field generated by the coherent transmitting transducer and that, because of the complete symmetry between transmit and receive modes, U_r represents the pressure field generated by the coherent transducer and aberrated by the RPS. We have

$$U_t(\vec{x}) = e^{(j\pi/\lambda F)|\vec{x}|^2} \int d\vec{X}\, O_t(\vec{X}) e^{(-2j\pi/\lambda F)\vec{x}\,\vec{X}}; \tag{32}$$

for a position $\vec{\delta}$ of the RPS,

$$U_r(\vec{x}, \vec{\delta}) = e^{(j\pi/\lambda F)|\vec{x}|^2} \int d\vec{X}\, O_r(\vec{X}) t(\vec{X} - \vec{\delta}) \cdot e^{(-2j\pi/\lambda F)\vec{x}\,\vec{X}}. \tag{33}$$

The directivity pattern in receive mode is no longer axisymmetric in $\vec{x}$ as $U_t(\vec{x})$. For a given $\vec{\delta}$, it may present

lobes that are not axially oriented and whose shape change with $\vec{\delta}$ [27].

In pulse echo mode, considering a scattering medium equivalent to a random mirror with reflectance $r(\vec{x})$, placed on the focal plane of the transducer, the complex echo signal can be written as

$$E(\vec{\delta}) = \int d\vec{x}\; r(\vec{x})\; U_t(\vec{x})\; U_r(\vec{x}, \vec{\delta}). \qquad (34)$$

B. Influence of the Screen Position

In our model, the random phase screen is placed on the front surface of the transducer. However, the more general case in which the screen can be placed anywhere between the transducer and its focal plane is also interesting. We now show that in the Fresnel approximation, our model is robust enough to predict the behavior of the system in the more general case.

Since the transmit and receive mode are symmetrical, the cases where the screen acts in transmission and in reception are equivalent. Consider a screen, acting in transmit mode, placed at a distance D from the transducer. A point $\vec{x}_2$ of its surface senses a field $U_i(\vec{x}_2)$. In the Fresnel approximation, we have

$$\begin{aligned} U_i(\vec{x}_2) &\propto O_t(\vec{x}_2) \exp\left(-j\frac{\pi}{\lambda F}|\vec{x}_2|^2\right) \\ &\quad \otimes \exp\left(j\frac{\pi}{\lambda D}|\vec{x}_2|^2\right) \\ &= \int d\vec{x}\; O_t(\vec{x}) \\ &\quad \cdot \exp\left[-j\frac{\pi}{\lambda}\left(\frac{|\vec{x}|^2}{F} - \frac{|\vec{x}_2 - \vec{x}|^2}{D}\right)\right] \\ &= \int d\vec{x}\; O_t(\vec{x}) \\ &\quad \cdot \exp\left[-j\frac{\pi}{\lambda}\left(\left|\vec{x} - \frac{F'}{D}\vec{x}_2\right|^2 - \frac{|\vec{x}_2|^2}{F - D}\right)\right] \\ &= \exp\left(-j\frac{\pi}{\lambda(F - D)}|\vec{x}_2|^2\right) \int d\vec{x}\; O_t(\vec{x}) \\ &\quad \cdot \exp\left(-j\frac{\pi}{\lambda F'}\left|\vec{x} - \frac{F'}{D}\vec{x}_2\right|^2\right), \end{aligned} \qquad (35)$$

where

$$\frac{1}{F} = \frac{1}{D} - \frac{1}{F}. \qquad (36)$$

The first term is a phase term that characterizes a transducer of focal length $(F - D)$. The second term is a Fresnel integral. It takes significant values for points located in the geometric shadow of the focused transducer. The incident pressure field on the focal plane is approximated by the field generated by an equivalent transducer placed just behind the RPS, and whose dimension fit in the geometric shadow of the real transducer (see Fig. 3). The equivalent transducer diameter is $(F - D)/F$ times the real diameter, its focal length is $(F - D)$.

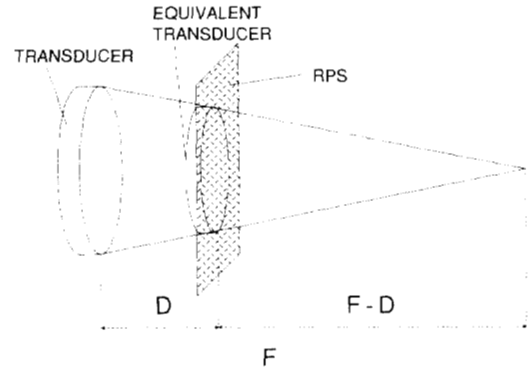

Fig. 3. Influence of RPS position. System in which the RPS is placed in beam of transducer rather than on its surface is equivalent to one where equivalent transducer is placed just behind RPS. Equivalent transducer fits in geometric shadow of real one; its focal point is real one.

As a conclusion, the case where the RPS is placed in the beam of the transducer can be treated just like the case where the RPS is placed on the transducer surface. We just need to consider the equivalent transducer.

C. Influence of the RPS on the Directivity

One limitation of incoherent transducers is their inability to achieve as good a directivity pattern as coherent transducers. The important parameter in the study of the directivity is the expectation of the intensity of the echo coming from a single diffuser placed at position $\vec{x}$ on the focal plane of the transducer. Since there is only one diffuser, the dependence of the echo as a function of the diffuser position is equal to the directivity pattern. For the system under investigation and, assuming the continuous wave case, the directivity pattern in transmit-receive mode, $D(\vec{x}, \vec{\delta})$, is the product of the directivity pattern of the transmitting focused transducer with the one of the receiving incoherent transducer. The intensity and amplitude approaches are conceptually equivalent [28]. However, it is mathematically simpler to work on the intensity. For this reason, we will use through the paper the intensity approach. We have

$$D(\vec{x}, \vec{\delta}) = U_t(\vec{x})\; U_r(\vec{x}, \vec{\delta}). \qquad (37)$$

Therefore the echo intensity for a diffuser located at position $\vec{x}$ is

$$\begin{aligned} |D(\vec{x}, \vec{\delta})|^2 &= D(\vec{x}, \vec{\delta})\, D^*(\vec{x}, \vec{\delta}) \\ &= |U_t(\vec{x})|^2 \iint d\vec{X}_1\, d\vec{X}_2\, O_r(\vec{X}_1) \\ &\quad \cdot O_r^*(\vec{X}_2)\, t(\vec{X}_1 - \vec{\delta})\, t^*(\vec{X}_2 - \vec{\delta}) \\ &\quad \cdot \exp\left[-j\frac{2\pi}{\lambda F}\vec{x}(\vec{X}_1 - \vec{X}_2)\right]. \end{aligned} \qquad (38)$$

Since the expectation is a linear operation, we have

$$\left\langle \left| D(\vec{x}, \vec{\delta}) \right|^2 \right\rangle_{\delta} = \left| U_t(\vec{x}) \right|^2 \iint d\vec{X}_1\, d\vec{X}_2\, O_r(\vec{X}_1)\, O_r^*(\vec{X}_2) \cdot R_t(\vec{X}_2 - \vec{X}_1) \exp\left[-j \frac{2\pi}{\lambda F} \vec{x}(\vec{X}_1 - \vec{X}_2) \right]. \tag{39}$$

We now define the change of variable

$$\vec{X}_3 = \vec{X}_2 - \vec{X}_1 \qquad \vec{X}_2 = \vec{X}_2 \tag{40}$$

for which the Jacobian is unity. We have

$$\begin{aligned} \left\langle \left| D(\vec{x}, \vec{\delta}) \right|^2 \right\rangle_{\delta} &= \left| U_t(\vec{x}) \right|^2 \iint d\vec{X}_2\, d\vec{X}_3\, O_r(\vec{X}_2 - \vec{X}_3) \cdot O_r^*(\vec{X}_2)\, R_t(\vec{X}_3)\, e^{j(2\pi/\lambda F)\vec{x}\,\vec{X}_3} \\ &= \left| U_t(\vec{x}) \right|^2 \int d\vec{X}_3\, R_t(\vec{X}_3)\, e^{j(2\pi/\lambda F)\vec{x}\,\vec{X}_3} \cdot \int d\vec{X}_2\, O_r(\vec{X}_2 - \vec{X}_3)\, O_r^*(\vec{X}_2) \\ &= \left| U_t(\vec{x}) \right|^2 \int d\vec{X}\, R_t(-\vec{X})\, O_r(\vec{X}) \otimes O_r^*(-\vec{X})\, e^{-j(2\pi/\lambda F)\vec{x}\,\vec{X}}, \end{aligned} \tag{41}$$

and, since the autocorrelation of the RPS is even, the expectation of the echo intensity is given by

$$\left\langle \left| D(\vec{x}, \vec{\delta}) \right|^2 \right\rangle_{\delta} = \left| U_t(\vec{x}) \right|^2 \mathrm{FT}\left[R_t(\vec{X})\, R_{Or}(\vec{X}) \right] \left(\vec{f} = \frac{\vec{x}}{\lambda F} \right) \tag{42}$$

where $R_{Or}(\vec{X})$ is the autocorrelation of the receiver aperture function. The directivity is the product of two terms. The first one, $|U_t|^2$ is the directivity of the coherent transmitting transducer. The second one, $\mathrm{FT}(R_t R_{Or})$ is the directivity (in the magnitude sense) of a coherent focused transducer whose aperture function is $R_t R_{Or}$.

Therefore, the important function, as far as directivity is concerned, is what we could call the equivalent aperture function of the incoherent transducer, defined as

$$O_{\mathrm{eq}}(\vec{X}) = R_t(\vec{X})\, R_{Or}(\vec{X}). \tag{43}$$

This function describes in a simple way the directivity properties of our system. One has to be careful when considering the equivalent aperture function to study the effects of the RPS on the directivity. The use of this function implies that we are interested in the directivity in the intensity sense.

Note that when the receiver and the transmitter are axisymmetric, the average directivity is also axisymmetric. This can be proved as follows: R_{Or}, R_t and U_t are axisymmetric, therefore, $\mathrm{FT}(R_t R_{Or})$ and the average directivity exhibit an axial symmetry. This remark shows that the RPS technique does not steer the ultrasound beam.

Directivity patterns can be estimated using computer simulations. Simulations were performed for a circular transducer with central frequency of 3.5 MHz, diameter of 19 mm, and focal length of 60 mm, and for different values of σ_t and σ_τ. The directivity patterns are shown in Fig. 4 where they are compared to the ideal directivity pattern of the coherent transducer. This figure shows how the directivity can be strongly reduced when $R_t(\vec{X})$ is narrow (i.e., when the coherence length of the RPS is short).

D. The Autocorrelation of the Echo

The idea in incoherent pulse-echo processing using a RPS is to obtain several images of the diffusing medium. It is hoped that these images will be uncorrelated and thus that it is possible to average out the speckle noise. In the following discussion, we study the autocorrelation of the echo with respect to the screen position, and we derive a necessary condition for the echoes to be uncorrelated.

Consider as before, a transducer and a RPS placed in front of an uncorrelated scattering medium. We have, for two positions, $\vec{\delta}_1$ and $\vec{\delta}_2$ of the RPS

$$E(\vec{\delta}_1)\, E^*(\vec{\delta}_2) = \iint d\vec{x}_1\, d\vec{x}_2\, r(\vec{x}_1)\, r^*(\vec{x}_2)\, U_t(\vec{x}_1)\, U_t^*(\vec{x}_2) \cdot U_r(\vec{x}_1, \vec{\delta}_1)\, U_r^*(\vec{x}_2, \vec{\delta}_2). \tag{44}$$

Therefore the autocorrelation of the echo, with respect to the position of the RPS, is

$$\left\langle E(\vec{\delta}_1)\, E^*(\vec{\delta}_2) \right\rangle_{\delta} = \iint d\vec{x}_1\, d\vec{x}_2\, r(\vec{x}_1)\, r^*(\vec{x}_2)\, U_t(\vec{x}_1)\, U_t^*(\vec{x}_2) \times \left\langle U_r(\vec{x}_1, \vec{\delta}_1)\, U_r^*(\vec{x}_2, \vec{\delta}_2) \right\rangle_{\delta}. \tag{45}$$

The expectation with respect to the medium of this last expression can be written as

$$\begin{aligned} \left\langle E(\vec{\delta}_1)\, E^*(\vec{\delta}_2) \right\rangle_{\delta,\,\mathrm{medium}} &= \iint d\vec{x}_1\, d\vec{x}_2 \left\langle r(\vec{x}_1)\, r^*(\vec{x}_2) \right\rangle_{\mathrm{medium}} \cdot U_t(\vec{x}_1)\, U_t^*(\vec{x}_2) \times \left\langle U_r(\vec{x}_1, \vec{\delta}_1)\, U_r^*(\vec{x}_2, \vec{\delta}_2) \right\rangle_{\delta} \\ &\propto \iint d\vec{x}_1\, d\vec{x}_2\, \delta(\vec{x}_1 - \vec{x}_2)\, U_t(\vec{x}_1)\, U_t^*(\vec{x}_2) \cdot \left\langle U_r(\vec{x}_1, \vec{\delta}_1)\, U_r^*(\vec{x}_2, \vec{\delta}_2) \right\rangle_{\delta} \\ &\propto \int d\vec{x}\, \left| U_t(\vec{x}) \right|^2 \left\langle U_r(\vec{x}, \vec{\delta}_1)\, U_r^*(\vec{x}, \vec{\delta}_2) \right\rangle_{\delta}. \end{aligned} \tag{46}$$

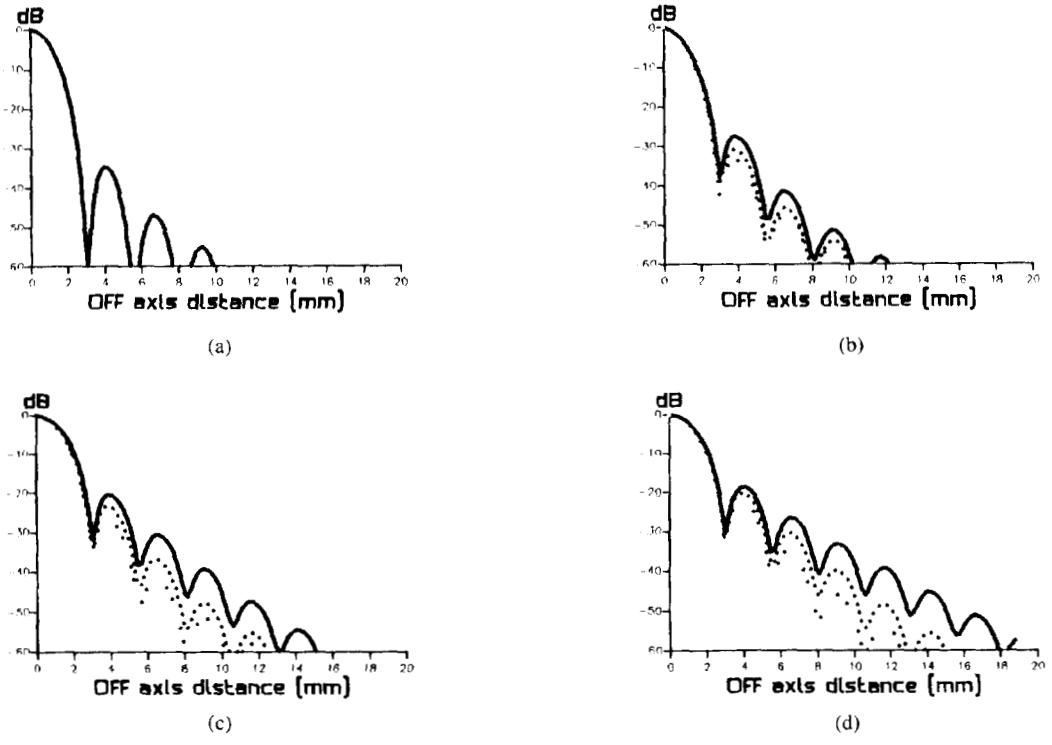

Fig. 4. Directivity pattern of the system in transmit-receive mode. Directivity is investigated for several configurations, ((b) σ_r = 0.2 T. (c) σ_r = 0.4 T. (d) σ_r = 0.6 T) and is compared to the one of the coherent transducer (a). σ_L is as follows: —— = 5 mm, · · · · · · = 8 mm, and · · · · · = 11 mm.

The term between brackets can be developed as

$$\langle U_r(\vec{x}, \vec{\delta}_1)\, U_r^*(\vec{x}, \vec{\delta}_2)\rangle_{\delta}$$

$$= \int\int d\vec{X}_1\, d\vec{X}_2\, R_t[\vec{X}_2 - \vec{X}_1 - (\vec{\delta}_2 - \vec{\delta}_1)] \cdot O_r(\vec{X}_1)\, O_r^*(\vec{X}_2) e^{-j(2\pi/\lambda F)\vec{x}(\vec{X}_1 - \vec{X}_2)}$$

$$= \int d\vec{X}\, R_t[\vec{X} - (\vec{\delta}_2 - \vec{\delta}_1)] R_{Or}(\vec{X}) e^{-j(2\pi/\lambda F)\vec{x}\,\vec{X}} \tag{47}$$

Therefore, the autocorrelation of the echo is

$$\langle E(\vec{\delta}_1)\, E^*(\vec{\delta}_2)\rangle_{\delta,\text{medium}}$$

$$= \int d\vec{x}\, |U_t(\vec{x})|^2\, \mathrm{FT}[R_t(\vec{X} - \vec{\delta})\, R_{Or}(\vec{X})] \cdot \left(\vec{f} = \frac{\vec{x}}{\lambda F}\right) \tag{48}$$

where $\vec{\delta} = \vec{\delta}_2 - \vec{\delta}_1$.

From this expression, it is clear that the autocorrelation is zero when, for all $\vec{X}$, the product $R_t(\vec{X} - \vec{\delta}_1)\, R_{Or}(\vec{X})$ is zero. This condition will be satisfied provided that both R_t and R_{Or} vanish as $\vec{X}$ increases infinitely and that the shift $\vec{\delta}_1$ between two positions of the screen is larger than half the sum of the widths of R_t and R_{Or}.

Fig. 5 shows the autocorrelation of the echo. Note that it does not vanish as the shift increases infinitely. This

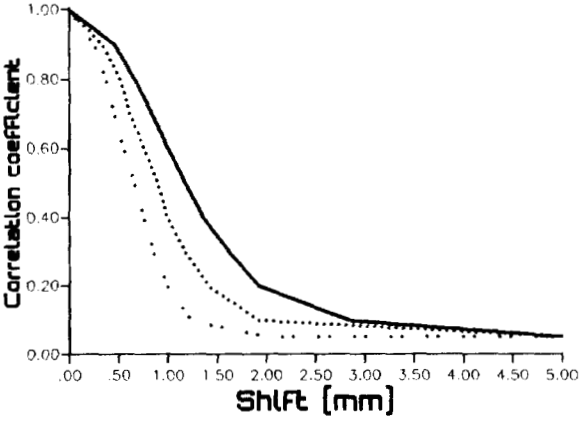

Fig. 5. Autocorrelation of echo. This function is investigated for σ_r = 0.6 T, and different σ_L. It is thinner when RPS correlation length is shorter.

may be due to the fact that the RPS autocorrelation does not vanish either. To obtain two almost uncorrelated echographic lines with a RPS placed on the surface of the transducer, we have to move it over a distance of the order of the half size of the receiving aperture. This implies large displacements that are unpracticable. However, if the screen is placed in the beam of the transducer, rather than on its surface, the configuration becomes equivalent to one in which the transducer diameter is equal to the beam width. Therefore, displacements of the order of half the beam diameter are required. If the RPS is on (or close to) the focal plane, the required displacement is very small.

Notice the relationships between the size of the previously-defined information grains and the shift for which the echoes are uncorrelated. When the RPS is totally incoherent (i.e., the width of its delay autocorrelation is zero), for any position of the RPS between the transducer and its focal plane, a shift of half the size of a grain yields uncorrelated echoes. This observation suggests that in general uncorrelated echoes may be obtained for RPS displacements of the order of half an information grain.

E. SNR Improvement

In this section, we study the theoretical limit for the SNR improvement. The SNR is defined as the ratio of the average magnitude (or intensity) to the root mean square deviation from the average.

$$\mathrm{SNR}_{\mathrm{magnitude}} = \frac{\langle |E| \rangle}{\sqrt{\langle |E|^2 \rangle - \langle |E| \rangle^2}}, \tag{49}$$

or

$$\mathrm{SNR}_{\mathrm{intensity}} = \frac{\langle |E|^2 \rangle}{\sqrt{\langle |E|^4 \rangle - \langle |E|^2 \rangle^2}}. \tag{50}$$

where the averaging operations are considered with respect to the medium (i.e., the average is estimated over a large number of position of the transducer).

In a classical pulse-echo system, the SNR of the magnitude detected signal is well known to be 1.91, while for the intensity detected signal it is 1.0. In our approach, the useful signal is the average over a set of RPS positions of the magnitude or intensity detected echographic signals. The new SNR is in the same way defined as

$$\mathrm{SNR}_{\mathrm{magnitude}} = \frac{\langle \langle |E| \rangle_{\mathrm{RPS}} \rangle_{\mathrm{medium}}}{\sqrt{\langle \langle |E| \rangle_{\mathrm{RPS}}^2 \rangle_{\mathrm{medium}} - \langle \langle |E| \rangle_{\mathrm{RPS}} \rangle_{\mathrm{medium}}^2}}, \tag{51}$$

or

$$\mathrm{SNR}_{\mathrm{intensity}} = \frac{\langle \langle |E|^2 \rangle_{\mathrm{RPS}} \rangle_{\mathrm{medium}}}{\sqrt{\langle \langle |E|^2 \rangle_{\mathrm{RPS}}^2 \rangle_{\mathrm{medium}} - \langle \langle |E|^2 \rangle_{\mathrm{RPS}} \rangle_{\mathrm{medium}}^2}}. \tag{52}$$

The numerator of the SNR is simply the expectation with respect to the medium and the RPS position of the echo intensity. The square of the denominator in the variance of the echo intensity. Its first term reads

$$\begin{aligned} &\langle \langle |E|^2 \rangle_{\mathrm{RPS}}^2 \rangle_{\mathrm{medium}} \\ &= \langle \langle I(\vec{X}, \vec{\delta}) \rangle_{\vec{\delta}}^2 \rangle_{\vec{X}} \\ &= \int d\vec{X} \left[\int d\vec{\delta}\, I(\vec{X}, \vec{\delta}) \right]^2 \\ &= \int d\vec{X} \iint d\vec{\delta}_1\, d\vec{\delta}_2\, I(\vec{X}, \vec{\delta}_1)\, I(\vec{X}, \vec{\delta}_2) \\ &= \iiint d\vec{\delta}_1\, d\vec{\delta}_2\, d\vec{X}\, I(\vec{X}, \vec{\delta}_1)\, I(\vec{X}, \vec{\delta}_2) \\ &= \langle I(\vec{X}, \vec{\delta}_1)\, I(\vec{X}, \vec{\delta}_2) \rangle_{\vec{\delta}_1, \vec{\delta}_2, \mathrm{medium}}. \end{aligned} \tag{53}$$

1) Expectation of the Echo Intensity: The expectation J of the echo intensity I is equal to the autocorrelation of the echo for $\Delta\vec{\delta} = \vec{0}$. It reads

$$\begin{aligned} J &= \int d\vec{x}\, \left| U_t(\vec{x}) \right|^2 \int d\vec{X}\, R_t(\vec{X})\, R_{Or}(\vec{X}) e^{-j(2\pi/\lambda F)\vec{x}\,\vec{X}} \\ &= \int d\vec{X}\, R_t(\vec{X})\, R_{Or}(\vec{X}) \int d\vec{x}\, \left| U_t(\vec{x}) \right|^2 e^{-j(2\pi/\lambda F)\vec{x}\,\vec{X}} \\ &= \int d\vec{X}\, R_t(\vec{X})\, R_{Or}(\vec{X})\, R_{Ot}(\vec{X}). \end{aligned} \tag{54}$$

2) SNR: The variance of the echo intensity is computed in the appendix. The SNR is given by

$$\mathrm{SNR} = \frac{\int d\vec{X}\, R_t(\vec{X})\, R_{Or}(\vec{X})\, R_{Ot}(\vec{X})}{\sqrt{\iiint\!\!\int d\vec{X}_1\, d\vec{X}_2\, d\vec{X}_3\, d\vec{X}_4\, R_t(\vec{X}_2 - \vec{X}_1)\, R_t(\vec{X}_4 - \vec{X}_3)\, O(\vec{X}_1)\, O^*(\vec{X}_2)\, O^*(\vec{X}_3)\, O(\vec{X}_4)\, R_{Or}(\vec{X}_1 - \vec{X}_3)\, R_{Or}(\vec{X}_2 - \vec{X}_4)}}. \tag{55}$$

Note that the SNR improvement depends only on the characteristics of the RPS and the transmitting and receiving apertures. In general, we cannot find a simpler analytic expression for the SNR. However, it can be computed with the use of computers. For the 1-D case, the denominator is a quadruple integral that requires 10^8 operations if we choose a resolution of $1/100$ of the receiving aperture diameter. In the 2-D case, with the same resolution, 10^{16} operations are required. This high number of operations make the computation in the 2-D case unpractical.

3) Limiting Case: Totally Incoherent RPS: In the limiting case of a totally incoherent RPS, a simple expression can be derived for the SNR. In that case, the autocorrelation function of the screen is proportional to a Dirac

function. Therefore, we have

$$\sigma_I^2 = \iint d\vec{X}_1\, d\vec{X}_2 \left|O_r(\vec{X}_1)\right|^2 \left|O_r(\vec{X}_2)\right|^2 R_{Ot}^2(\vec{X}_1 - \vec{X}_2)$$
$$= \int d\vec{X}_3\, R_{Ot}^2(\vec{X}_3) \int d\vec{X}_1 \left|O_r(\vec{X}_1)\right|^2 \left|O_r(\vec{X}_1 - \vec{X}_3)\right|^2. \quad (56)$$

Now, since

$$\left|O_r(\vec{X})\right|^2 = O_r(\vec{X}), \quad (57)$$

σ_I^2 reduces to

$$\sigma_I^2 = \int d\vec{X}\, \left(R_{O_t}(\vec{X})\right)^2 R_{Or}(\vec{X}). \quad (58)$$

A simpler expression can be obtained for J:

$$J = \int d\vec{X}\, \delta(\vec{X})\, R_{Or}(\vec{X})\, R_{Ot}^*(\vec{X})$$
$$= R_{Or}(\vec{0})\, R_{Ot}^*(\vec{0}). \quad (59)$$

Since the receiving aperture is not modulated, the above expression reduces to the product of the areas of transmission and reception:

$$J = A_t \times A_r. \quad (60)$$

And finally, the SNR is

$$\mathrm{SNR} = \frac{A_t \times A_r}{\sqrt{\int d\vec{X}\, \left(R_O(\vec{X})\right)^2 R_{Or}(\vec{X})}}. \quad (61)$$

a) 1-D Aperture Functions: In the special case of 1-D aperture functions, an analytic expression can be obtained:

$$A_r \geq A_t\ \mathrm{SNR} = \sqrt{\frac{6}{Y(4 - Y)}}; \qquad Y = \frac{A_t}{A_r}. \quad (62)$$

The SNR is plotted in Fig. 6 against the ratio of the transmitting aperture to the receiving one. Note that the maximum achievable SNR improvement when the same aperture is used in transmit and receive modes is $\sqrt{2}$.

b) 2-D Aperture Functions: The case of rectangular apertures can be deduced via a squaring operation from the 1-D case, for this reason, it won't be considered further.

The case of circular apertures is interesting because it corresponds to realistic implementations of the aforementioned system. The autocorrelation of a circular aperture with diameter d_0 is given by (see [25, p. 35])

$$R_O(r) = \frac{d_0^2}{2}\left[\cos^{-1}\frac{r}{d_0} - \frac{r}{d_0}\sqrt{1 - \left(\frac{r}{d_0}\right)^2}\right] \qquad r \leq d_0$$
$$= 0 \qquad \text{otherwise.} \quad (63)$$

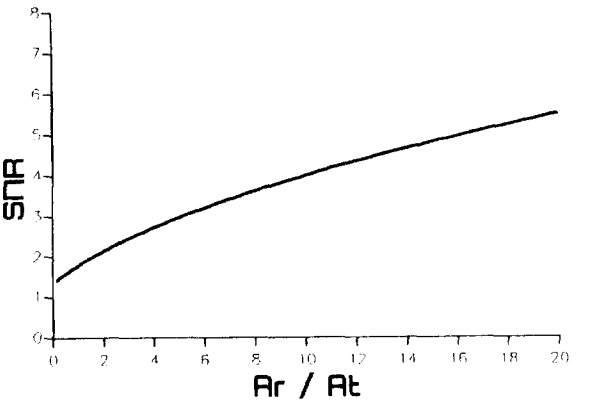

Fig. 6. SNR improvement with 1-D apertures.

The aperture autocorrelation can be rewritten as

$$R_O(r) = d_0^2 f\left(\frac{r}{d_0}\right) \quad (64)$$

to emphasize its dependence on the ratio r/d_0. If we assume that $d_t \leq d_r$, σ_I can be written as

$$\sigma_I = d_r^2\, d_t^6\, 2\pi \int r\, dr\, f^2(r)\, f\left(r\frac{d_t}{d_r}\right). \quad (65)$$

Thus we show that the SNR is a function of $Y = d_r/d_t$, the ratio of the aperture diameters:

$$\mathrm{SNR} = \frac{Y\pi^{3/2}}{\sqrt{2\int r\, dr\, f^2(r)\, f\left(\frac{r}{Y}\right)}}. \quad (66)$$

The SNR is plotted in Fig. 7 against the ratio of the transmitting aperture to the receiving one. Note that the maximum achievable SNR improvement when the same aperture is used in transmit and receive modes is 1.94. The SNR improvements obtained with 2-D apertures are always larger than with 1-D apertures.

The aforementioned result regarding the maximum SNR improvement was derived for a coherent transducer coupled with a totally incoherent RPS, a configuration that yields the same echographic signal as a totally incoherent transducer such as those made of CdS. Therefore, no matter which incoherent process is used, we cannot achieve a better SNR improvement than what is predicted here. If the transmitting and receiving areas are the same, the SNR improvement will always be lower than 1.94.

This result explains why a maximal SNR improvement of less than 2.0 was obtained for the "Maltese Cross Processor" [19].

4) General Case: As we said earlier, the computation of the SNR improvement in the general case requires the computation of a quadruple integral. This was performed for linear apertures (1-D case) with the use of computers for relative sizes of transmitting and receiving apertures varying from 1.0 to 5.0. The results for several values for σ_T and σ_L are summarized in Fig. 8. These results show that with a σ_T of 0.4 T, improvements very close to the

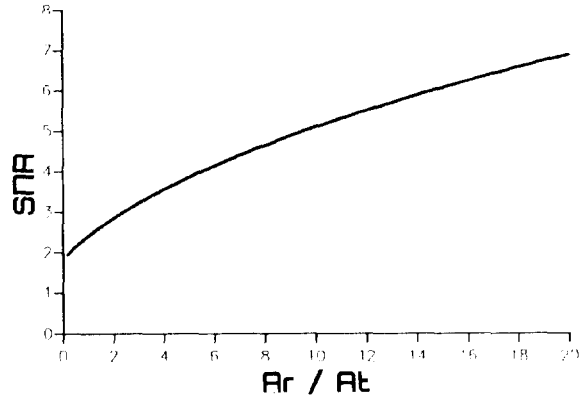

Fig. 7. SNR improvement with 2-D apertures.

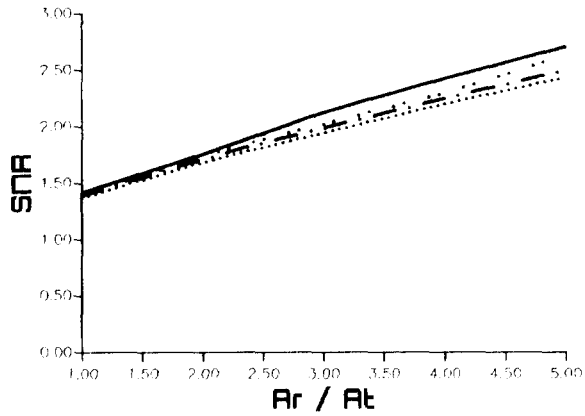

Fig. 8. SNR improvement for general case. SNR improvement obtained in 1-D case for nonideal (not totally incoherent) RPS is investigated for σ_τ of 0.4 T for different values of σ_L. It is compared to maximum achievable SNR improvement in incoherent processing. σ_L is as follows: —— = 11 mm; — — — = 8 mm; · · · · · · = 5 mm.

theoretical limit can be achieved for quite large σ_L (between 4 and 7 mm). These values for σ_L correspond to RPS grains of the order of half the transducer size. That is, RPS grains of the same size as the backscattered information grains.

These results suggest that a good configuration that maximizes the SNR without too much loss in directivity involves a RPS whose grains are well matched to the backscattered information grains. In the case of the 1-D focused transducer, the information grains are about two times smaller than the transmitting transducer.

Equivalent results are expected for the 2-D case. As long as the RPS grains are well matched to the information grains, we can expect SNR improvements very close to the theoretical prediction.

5) RPS in Transmit and Receive Modes: The case where the RPS is present in both the transmit and receive modes is very difficult to analyze theoretically because it involves eighth-order statistics of the RPS transmittance. However, several results derived for the simpler configuration can be generalized.

We can consider that the main effect of the RPS in transmit mode is to distord the ultrasound beam. This effect is quantified in [27]. The incident beam has lobes whose shape and direction change with the RPS position. In average, the directivity of the system is equivalent to the one of a transducer with aperture function O_{eq} defined as

$$O_{eq} = R_t \cdot R_{Ot}. \tag{67}$$

Fig. 9 shows the equivalent transmitting aperture for two different RPSs. We can readily see that when the transmittance autocorrelation function is narrow, the equivalent aperture is equal (within a constant factor) to the transmittance autocorrelation itself. This means that the equivalent transmitting aperture has the size of a RPS grain. That is, the equivalent transmit area is a function of σ_L and σ_τ.

In the case where the RPS transmittance autocorrelation is not narrow enough, an equivalent aperture area can be defined as the area of the focused coherent transducer that would have the same directivity at, for example, −25 dB.

Let's consider that the approximation for which the equivalent aperture is a function of σ_L and of σ_τ is true. For σ_τ = 0.4 T, the width of the RPS autocorrelation function is roughly equal to σ_L. The diameter of the equivalent transmitting transducer is thus roughly equal to σ_L. Therefore, the SNR improvement is a function of σ_L/D, where D is the true diameter of the transducer that acts in both transmit and receive modes. The directivity in T/R mode is a function of σ_L. Fig. 10 shows the SNR improvement as a function of σ_L/D as well as the −25 dB width of the directivity in T/R mode as a function of σ_L. This figure summarizes the compromise between directivity and SNR improvement.

V. Conclusion

This paper shows the theoretical limits of incoherent transducers through the concept of information grains. The SNR improvement we can achieve depends on the number of received information grains. The information grain size depends on the transmit beam width. The wider the incident beam, the smaller the information grains, the more grains we can receive on a given surface, and thus the higher the SNR.

We have presented a new processing approach of pulse-echo signals that yields spatial incoherence. In this technique there is no need to use power sensitive transducers, to sample the backscattered field, or to divide the receiving apertures into subapertures. This technique consists in using a coherent transducer that covers the entire receiving aperture and in a moving random phase screen placed in front of it. The second-order statistics of the RPS (RPS grain size) need to be well matched to the size of the backscattered information grains. This technique optimizes the compromise between directivity and SNR improvement. In this paper we show that a totally incoherent transducer is equivalent to a special case of our system. The properties of our system, as far as directivity and SNR improvement are concerned, are also studied. In

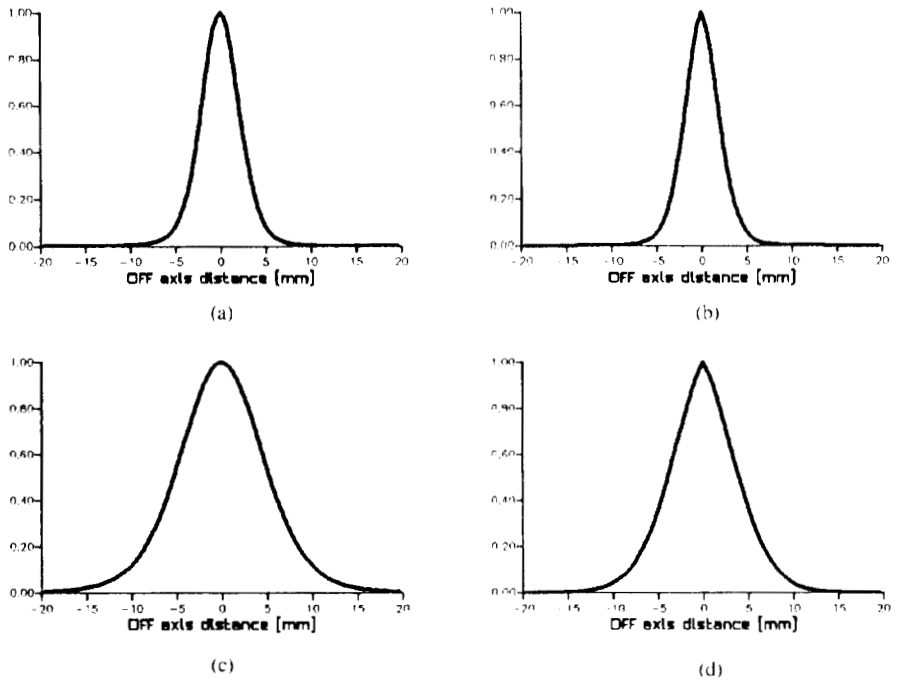

Fig. 9. Equivalent transmit aperture functions. Equivalent transmit aperture function is given for two values for σ_L (5 and 11 mm) and a σ_r of 0.4 T, for 19-mm diameter transducer. It is compared to RPS autocorrelation function. When RPS autocorrelation function is narrow (σ_L = 5 mm) (a), the equivalent aperture width is of the same order (b). When the RPS autocorrelation is wide (σ_L = 11 mm) (c), the equivalent aperture is narrower (d).

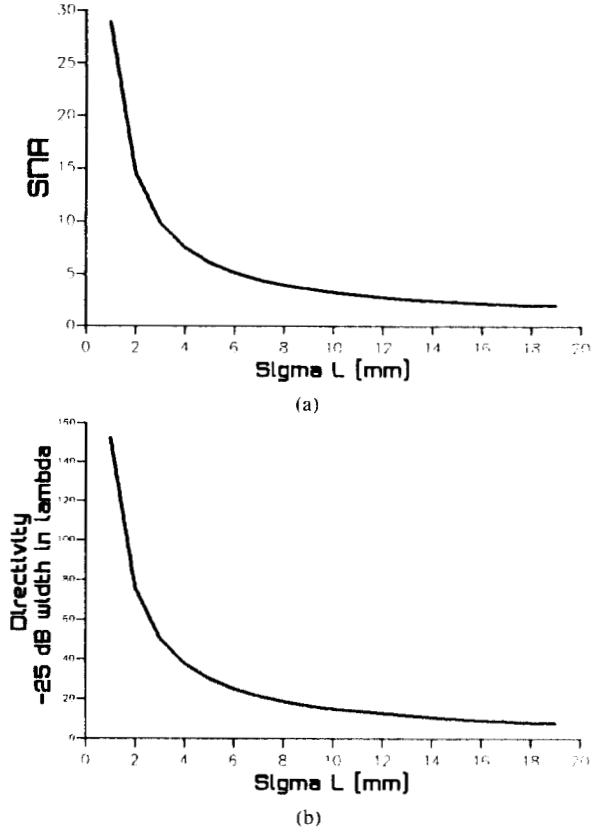

Fig. 10. SNR improvement (a) and directivity (b) for RPS in T/R mode: When RPS is present in both modes, the SNR and directivity are functions of transducer diameter, σ_r and σ_L. Here, they are investigated for σ_r of 0.4 T, diameter of 19 mm and aperture number of f/4. Note that very high SNR (close to 30) can be achieved, at cost of poor directivity.

[27] we show experimental results in speckle reduction obtained with this technique.

Even though this technique for incoherent processing is simple to implement, it involves the translation of a screen in front of the transducer. The translating nature of the screen makes the design of compact probes impossible. We are currently investigating a rotating configuration that allows a miniaturization of the probes.

Appendix A

A. Modelization of the Scattering Medium

The scattering medium is modeled as a random distribution of scatterers located in the insonified volume. In pulse–echo processing, the scattering volume is divided into elementary slices whose thickness is equal to the resolution cell.

In a monochromatic approach, an elementary slice can be described by a 2-D random mirror of complex reflectance $r(\vec{x})$ such that

$$P_r(\vec{x}) = r(\vec{x})\, P_i(\vec{x}), \tag{68}$$

where $\vec{x}$ is the position in the slice, and where $P_i(\vec{x})$ and $P_r(\vec{x})$ are respectively the incident and reflected complex pressure fields at the position $\vec{x}$ in the slice. This description is justified as follows.

Consider an elementary slice of the scattering medium. It can be decomposed into a large number of infinitely narrow, axially oriented, elementary cylinders (see Fig. 11).

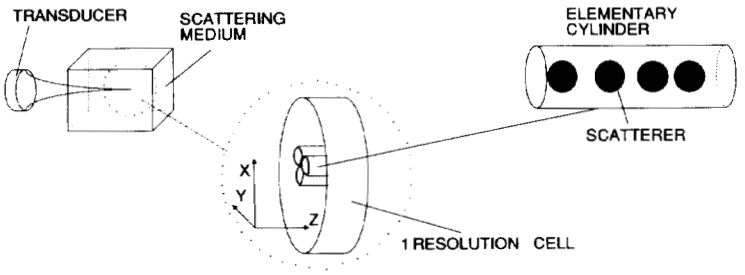

Fig. 11. Modelization of the scattering medium.

Consider now the pressure field in one elementary cylinder located at position $\vec{x}_0$ ($\vec{x}_0 = (x_0, y_0, z_0)$) in the slice. The incident pressure field in that cylinder at the depth z (coordinates $\vec{x} = (x_0, y_0, z)$) is expressed in terms of the incident field in $\vec{x}_0$:

$$P_i(\vec{x}) = P_i(\vec{x}_0)e^{-jk(z-z_0)}, \tag{69}$$

where k is the wave number ($k = \omega/c$). Now if a scatterer of scattering strength ρ is present at that depth, the reflected field is given by

$$P_r(\vec{x}) = \rho P_i(\vec{x}_0)e^{-jk(z-z_0)}. \tag{70}$$

Considering backwards propagation, the reflected field at $\vec{x}_0$ due to that scatterer is

$$P_r(\vec{x}_0, \vec{x}) = \rho P_i(\vec{x}_0)e^{-2jk(z-z_0)}. \tag{71}$$

Therefore, since all the scatterers are identical, the reflected field at $\vec{x}_0$ is

$$P_r(\vec{x}_0) = \rho \sum_{i \in \text{scatterers}} e^{-2jk(z_i-z_0)}P_i(\vec{x}_0). \tag{72}$$

The reflectance is thus given by

$$r(\vec{x}) = \rho \sum_{i \in \text{scatterers}} e^{-2jk(z_i-z_0)}. \tag{73}$$

This summation can be seen as the result of a random walk on a plane. It is well known that for a large number of scatterers, (typically more than 100), the real and imaginary parts of $r(\vec{x})$ are jointly Gaussian random variables with zero mean and same variance. Moreover, if the scattering microstructure is uncorrelated, the autocorrelation of $r(\vec{x})$ is proportional to a Dirac function.

B. Variance of the Echo Intensity

The variance σ_I^2 of the echo intensity is

$$\sigma_I^2 = \langle I(\vec{X}, \vec{\delta}_1)\, I(\vec{X}, \vec{\delta}_2)\rangle_{\vec{\delta}_1, \vec{\delta}_2, \text{medium}} - J^2. \tag{74}$$

We have

$$I(\vec{\delta}_1)\, I^*(\vec{\delta}_2) = \left|E(\vec{\delta}_1)\right|^2\left|E^*(\vec{\delta}_2)\right|^2 = \left|\int d\vec{x}\; U_t(\vec{x})\, U_r(\vec{x}, \vec{\delta}_1)\, r(\vec{x})\right|^2 \cdot \left|\int d\vec{x}\; U_t(\vec{x})\, U_r(\vec{x}, \vec{\delta}_2)\, r(\vec{x})\right|^2. \tag{75}$$

Therefore the expectation with respect to the medium yields

$$\begin{aligned}\langle I(\vec{\delta}_1)\, I^*(\vec{\delta}_2)\rangle_{\text{medium}} &= \iiiint d\vec{x}_1\, d\vec{x}_2\, d\vec{x}_3\, d\vec{x}_4 \\ &\cdot \langle r(\vec{x}_1)\, r^*(\vec{x}_2)\, r(\vec{x}_3)\, r^*(\vec{x}_4)\rangle_{\text{medium}} \\ &\times U_t(\vec{x}_1)\, U_t^*(\vec{x}_2)\, U_t(\vec{x}_3)\, U_t^*(\vec{x}_3) \\ &\times U_r(\vec{x}_1, \vec{\delta}_1)\, U_r^*(\vec{x}_2, \vec{\delta}_1)\, U_r(\vec{x}_3, \vec{\delta}_2) \\ &\cdot U_r^*(\vec{x}_4, \vec{\delta}_2).\end{aligned} \tag{76}$$

Since the reflectance is an uncorrelated Gaussian random variable, the term between brackets can be rewritten as

$$\begin{aligned}\langle r_1 r_2^* r_3 r_4^*\rangle &= \langle r_1 r_2^*\rangle\langle r_3 r_4^*\rangle + \langle r_3 r_2^*\rangle\langle r_1 r_4^*\rangle \\ &= \delta(\vec{x}_2 - \vec{x}_1)\,\delta(\vec{x}_4 - \vec{x}_3) \\ &\quad + \delta(\vec{x}_2 - \vec{x}_3)\,\delta(\vec{x}_4 - \vec{x}_1).\end{aligned} \tag{77}$$

Therefore the previous expression yields

$$\begin{aligned}\langle I(\vec{\delta}_1)\, I^*(\vec{\delta}_2)\rangle_{\text{medium}} &= \iint d\vec{x}_1\, d\vec{x}_2 \left|U_t(\vec{x}_1)\right|^2\left|U_r(\vec{x}_1, \vec{\delta}_1)\right|^2\left|U_t(\vec{x}_2)\right|^2 \\ &\cdot \left|U_r(\vec{x}_2, \vec{\delta}_2)\right|^2 + \iint d\vec{x}_1\, d\vec{x}_2 \\ &\cdot \left|U_t(\vec{x}_1)\right|^2\left|U_t(\vec{x}_2)\right|^2 \\ &\cdot U_r(\vec{x}_1, \vec{\delta}_1)\, U_r^*(\vec{x}_2, \vec{\delta}_1)\, U_r(\vec{x}_2, \vec{\delta}_2) \\ &\cdot U_r^*(\vec{x}_1, \vec{\delta}_2).\end{aligned} \tag{78}$$

The expectation with respect to $\vec{\delta}_1$ and $\vec{\delta}_2$ of the first integral is equal to J^2. Therefore the variance of the echo

intensity reduces to

$$\sigma_I^2 = \iint d\vec{x}_1\, d\vec{x}_2 \left|U_t(\vec{x}_1)\right|^2 \left|U_t(\vec{x}_2)\right|^2 \cdot \left|\left\langle U_r(\vec{x}_1, \vec{\delta})\, U_r^*(\vec{x}_2, \vec{\delta})\right\rangle_{\vec{\delta}}\right|^2$$

$$= \iint d\vec{x}_1\, d\vec{x}_2 \left|U_t(\vec{x}_1)\right|^2 \left|U_t(\vec{x}_2)\right|^2 \cdot \left|\iint d\vec{X}_1\, d\vec{X}_2\, R_t(\vec{X}_2 - \vec{X}_1)\, O_r(\vec{X}_1)\, O_r^*(\vec{X}_2) \cdot \exp\left[-j2\frac{\pi}{\lambda F}(\vec{x}_1\vec{X}_1 - \vec{x}_2\vec{X}_2)\right]\right|^2$$

$$= \iint d\vec{x}_1\, d\vec{x}_2 \left|U_t(\vec{x}_1)\right|^2 \left|U_t(\vec{x}_2)\right|^2 \cdot \iiiint d\vec{X}_1\, d\vec{X}_2\, d\vec{X}_3\, d\vec{X}_4\, O_r(\vec{X}_1) \cdot O_r^*(\vec{X}_2)\, O_r^*(\vec{X}_3) \cdot O_r(\vec{X}_4)\, R_t(\vec{X}_2 - \vec{X}_1)\, R_t^*(\vec{X}_4 - \vec{X}_3) \cdot \exp\left[-j2\frac{\pi}{\lambda F}(\vec{x}_1(\vec{X}_1 - \vec{X}_3) - \vec{x}_2(\vec{X}_2 - \vec{X}_4))\right]$$

$$= \iiiint d\vec{X}_1\, d\vec{X}_2\, d\vec{X}_3\, d\vec{X}_4\, O_r(\vec{X}_1) \cdot O_r^*(\vec{X}_2)\, O_r^*(\vec{X}_3) \cdot O_r(\vec{X}_4)\, R_t(\vec{X}_2 - \vec{X}_1)\, R_t(\vec{X}_4 - \vec{X}_3) \cdot \iint d\vec{x}_1\, d\vec{x}_2 \left|U_t(\vec{x}_1)\right|^2 \left|U_t(\vec{x}_2)\right|^2 \cdot \exp\left[-j2\frac{\pi}{\lambda F}(\vec{x}_1(\vec{X}_1 - \vec{X}_3) - \vec{x}_2(\vec{X}_2 - \vec{X}_4))\right]$$

$$= \iiiint d\vec{X}_1\, d\vec{X}_2\, d\vec{X}_3\, d\vec{X}_4\, R_t(\vec{X}_2 - \vec{X}_1) \cdot R_t(\vec{X}_4 - \vec{X}_3)\, O_r(\vec{X}_1)\, O_r^*(\vec{X}_2)\, O_r^*(\vec{X}_3) \cdot O_r(\vec{X}_4)\, R_{Ot}(\vec{X}_1 - \vec{X}_3)\, R_{Ot}(\vec{X}_2 - \vec{X}_4). \quad (79)$$

References

[1] J. M. Reid, "The measurement of scattering" in *Tissue Characterization with Ultrasound CRC*, J. F. Greenleaf, Ed., 1986, pp. 81–115.

[2] J. A. Campbell and R. C. Waag, "Measurement of calf liver ultrasonic differential and total scattering cross sections," *J. Acoust. Soc. Amer.*, vol. 75, pp. 603–611, 1984.

[3] P. H. Johnston and J. G. Miller, "Phase insensitive detection for measurement of backscattered ultrasound," *IEEE Trans. Ultrason. Ferroelec. Freq. Contr.*, vol. UFFC-33, pp. 713–721, 1986.

[4] R. Kuc, "Parametric estimation of the acoustic attenuation coefficient slope for soft tissues," *IEEE Ultrason. Symp. Proc.*, 1976, pp. 44–47.

[5] K. J. Parker, R. M. Lerner, and R. C. Waag, "Attenuation of ultrasound: Magnitude and frequency dependence for tissue characterization," *Radiology*, vol. 153, pp. 785–788, 1984.

[6] P. Laugier, G. Berger, and M. Fink, "Correction of diffraction for focused transducers for in vivo frequency dependent attenuation measurement," *Ultrason. Imaging*, vol. 9, pp. 248–260, 1987.

[7] C. B. Burckhardt, "Speckle in ultrasound B-mode scans," *IEEE Trans. Sonics Ultrason.*, vol. SU-25, pp. 1–6, 1978.

[8] J. C. Abott and F. L. Thurstone, "Acoustic speckle: Theory and experimental analysis," *Ultrason. Imaging*, vol. 1, pp. 303–324, 1979.

[9] R. F. Wagner, S. W. Smith, J. M. Sandrik, and H. Lopez, "Statistics of speckle in ultrasound B-scans," *IEEE Trans. Sonics Ultrason.*, vol. SU-30, pp. 156–163, 1983.

[10] R. F. Wagner, M. F. Insana, and S. W. Smith, "Fundamental correlation lengths of coherent speckle in medical ultrasonic images," *IEEE Trans. Ultrason. Ferroelect. Freq. Contr.*, vol. 35, pp. 34–44, 1988.

[11] J. W. Goodman, "Statistical properties of laser sparkle patterns," Stanford Electronics Laboratory Tech. Rep. No. 2303-1, 1963.

[12] ——, "Statistical properties of laser speckle patterns," in *Laser Speckle and Related Phenomena*, J. C. Dainty, Ed. Berlin: Springer Verlag, 1975, pp. 9–75.

[13] D. T. Kuan, A. A. Sawshuk, T. C. Strand, and P. Chavel, "Adaptive restoration of images with speckle," *IEEE Trans. Acoust. Speech Signal Processing*, vol. ASSP-35, pp. 373–382, 1982.

[14] G. E. Trahey, S. W. Smith, and O. T. von Ramm, "Speckle pattern correlation with lateral aperture translation: Experimental results and implication for spatial compounding," *IEEE Trans. Ultrason. Ferroelec. Freq. Contr.*, vol. 33, pp. 257–264, 1986.

[15] D. P. Shattuck and O. T. von Ramm, "Compound scanning with a phased array," *Ultrason. Imaging*, vol. 4, pp. 93–107, 1982.

[16] M. O'Donnell and S. D. Silverstein, "Optimum displacement for compound image generation in medical ultrasound," *IEEE Trans. Ultrason. Ferroelec. Freq. Contr.*, vol. 35, pp. 470–476, 1988.

[17] R. L. Galloway, B. A. McDermott, and F. L. Thurstone, "A frequency diversity process for speckle reduction in real time ultrasonic images," *IEEE Trans. Ultrason. Ferroelec. Freq. Contr.*, vol. 35, pp. 45–49, 1988.

[18] H. E. Melton, Jr., and P. A. Magnin, "A-mode speckle reduction with compound frequencies and compound bandwidths," *Ultrason. Imaging*, vol. 6, pp. 159–173, 1984.

[19] S. W. Smith and O. T. von Ramm, "The Maltese cross processor: Speckle reduction for circular transducers," *Ultrason. Imaging*, vol. 10, pp. 153–170, 1988.

[20] J. S. Heyman, "Phase insensitive acoustoelectric transducers," *J. Acoust. Soc. Amer.*, vol. 64, pp. 1370–1376, 1986.

[21] M. Fink, F. Cancre, C. Soufflet, and D. Beudon, "Attenuation estimation and speckle reduction with random phase transducers," *Proc. IEEE Ultrason. Symp.*, 1987, pp. 951–956.

[22] T. Sato, S. Wadaka, J. Ishii, and T. Sunda, "A new ultrasonic imaging system by using a rotating random phase disk and power spectral and third order correlation analysis," *Acoustical Holography*, vol. 7, pp. 167–178, 1977.

[23] U. Röder, C. Scherg, and H. Brettel, "Coherence and noise in ultrasonic transmission imaging," *Acoustical Imaging*, vol. 10, pp. 131–142, 1982.

[24] J. W. Goodman, *Introduction to Fourier Optics*. New York: McGraw-Hill, 1968.

[25] A. Papoulis, *Systems and Transforms with Applications in Optics*. New York: McGraw-Hill, 1968.

[26] M. O'Donnell, "Quantitative ultrasonic backscatter measurements in the presence of phase distortions," *J. Acoust. Soc. Amer.*, vol. 72, pp. 1719–1725, 1982.

[27] P. Laugier, M. Fink, and S. Abouelkaram, "The random phase transducer: A new technique for incoherent processing. Experimental results," *IEEE Trans. Ultrason. Ferroelec. Freq. Contr.*, this issue, pp. 70–78.

[28] S. M. Gehlbach, "Pulse reflection imaging and acoustic speckle," Ph.D. dissertation, Stanford University, Stanford, CA, Mar. 1983.

Mathias Fink was born in Grenoble, France, in 1945. He received the DEA degree in solid-state physics in 1968 and the diplome de Doctorat de 3ème cycle in 1970 from Paris University. In 1978 he received the Doctorat ès-sciences degree in Acoustics from University Pierre et Marie Curie, Paris.

From 1973 to 1979 he has worked on ultrasonic imaging with P. Alais, focusing with linear arrays and diffraction impulse theory. Since 1979 he has continued his research activities in Medical Ultrasound and in Nondestructive evaluation.

From 1981 to 1984 he has been Professor of Acoustics at Strasbourg University. Since 1984 he is Professor at Paris University. He served as a consultant to the L.E.P. since 1979. His research activities are in the development of novel techniques for speckle reduction, attenuation estimation, focusing in inhomogeneous media and nondestructive evaluation of scattering media (composite material, steel, titanium).

Raoul Mallart was born in 1965 in Madrid, Spain. He graduated from Ecole Superieure d'Electricité Gif sur Yvette, France, in 1987. He received the Master of Science in biomedical engineering from the University of Houston, Houston, TX, in 1988. He is currently working towards his Doctorat d'automatique et traitement du signal at Université Paris XI, Paris, France.

He is currently with the Groupe de Physique des Solides de l'ENS, Université Paris 7, Paris, France, with Professor Fink and with the Laboratoires d'Electronique, Philips.

His current research interest include incoherent processing technique of pulse echo signals and correction of sound speed fluctuations in echographic imaging.

F. Cancre, photograph and biography not available at time of publication.